processes

MDPI

Review

A Review of the Measurement of the Multiphase Slug Frequency

Ronaldo Luís Höhn, Abderraouf Arabi *, Youssef Stiriba and Jordi Pallares

Departament d'Enginyeria Mecànica, Universitat Rovira i Virgili, Av. Països Catalans 26, 43007 Tarragona, Spain; ronaldoluis.hohn@urv.cat (R.L.H.); youssef.stiriba@urv.cat (Y.S.); jordi.pallares@urv.cat (J.P.)
* Correspondence: abderraouf.arabi@urv.cat; Tel.: +34-666-111-569

Abstract: The slug frequency (SF), which refers to the number of liquid slugs passing through a pipe during a specific time, is an important parameter for characterizing the multiphase intermittent flows and monitoring some process involving this kind of flow. The simplicity of the definition of SF contrasts with the difficulty of correctly measuring it. This manuscript aims to review and discuss the various techniques and methods developed to determine the slug frequency experimentally. This review significantly reveals the absence of a universal measurement method applicable to a wide range of operating conditions. Thus, the recourse to recording videos with high-speed cameras, which can be used only at a laboratory scale, remains often necessary. From the summarized state-of-the-art, it appears that correctly defining the threshold values for detecting the liquid slugs/elongated bubbles interface from physical parameters time series, increasing the applicability of instrumentations at industrial scales, and properly estimating the uncertainties are the challenges that have to be faced to advance in the measurement of SF.

Keywords: multiphase flow; intermittent flow; slug flow; slug frequency; measurement techniques

Citation: Höhn, R.L.; Arabi, A.; Stiriba, Y.; Pallares, J. A Review of the Measurement of the Multiphase Slug Frequency. *Processes* **2024**, *12*, 2500. https://doi.org/10.3390/pr12112500

Academic Editor: Blaž Likozar

Received: 7 October 2024
Revised: 6 November 2024
Accepted: 7 November 2024
Published: 11 November 2024

1. Introduction

The multiphase flow in pipes, especially the gas–liquid two-phase, has been intensively studied. This can be explained by their occurrence in several industrial systems such as petroleum and gas production, power generation, airlift pumping, heat exchangers, chemical processing, aerospace engineering, paper production, and medical devices [1–5]. The main characteristic of these flows is the presence of several flow regimes or flow patterns [6]. The existence region of each flow regime can be detected using flow transition models or flow maps [7]. The slug flow, or intermittent flow, refers to the flow regime where two flow structures (liquid slug and elongated bubble) flow alternatively, as shown in Figure 1 taken from [8]. A slug unit is constituted by a liquid slug and an elongated bubble. As shown in Figure 1, the elongated bubbles flow over the liquid film horizontally, and where the pipe inclination is below 45°. For $\theta \geq 45°$ and due to the effect of buoyancy, the elongated bubbles flow in the center of the pipe surrounded by the liquid film. Note that the elongated bubble is referred to as a Taylor bubble in these cases. In Figure 1, U_{TB}, L_{LS}, L_{TB}, and L_{SU} refer to the translational velocity of the elongated bubble, liquid slug length, elongated bubble length, and slug unit length, respectively. The slug flow occurs in all multiphase systems constituted by one gas and one liquid at least. This flow regime is characterized by intrinsic parameters, such as slug frequency (SF). This refers to the number of liquid slugs passing by one point during a fixed time period.

Since the pioneering works carried out in Hubbard's thesis [9] and Gregory and Scott [10], SF intensively has been studied in the literature. Such interest has come from its great importance in the industry. Indeed, it is employed as a parameter for closing and informing the slug models used to predict the different design parameters, such as pressure drop [11]. In addition, the pipeline structural instability, wellhead pressure fluctuations, severe pipe corrosion, and FIV (flow-induced vibration) response are directly related to SF [12,13]. The monitoring of SF in several processes is also important to assess the hazards

and avoid accidents [14]. The difficulty of properly modeling SF explains the popular recourse to the empirical approach for predicting it [15]. These reasons also explain the need to correctly measure SF [11].

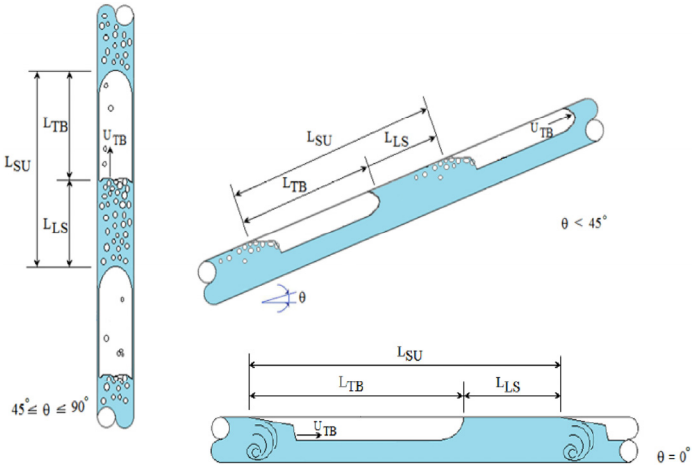

Figure 1. Schematic presentation of the slug flow for different pipe inclination range. The intrinsic slug parameters are also displayed. Reprinted from [8]. Reprinted from *Flow Measurement and Instrumentation*, vol. 72, O. Cazarez-Candia, O.C. Benítez-Centeno, Comprehensive experimental study of liquid-slug length and Taylor-bubble velocity in slug flow, page 2, Copyright © 2020, with permission from Elsevier.

Based on its definition, SF was measured in the pioneering works by counting the number of liquid slugs passing through a single cross-sectional area of pipe during a specific time period. This can be achieved by direct visual observation of flow with a simple stopwatch in the hand or by recourse to a camera. Through the time, different experimental techniques were used or specially developed to measure the SF, whether for studying this parameter at the laboratory scale or for active control at the industrial/field scale. This advancement was in line with the increasing innovations in the area of multiphase flow measurement [16]. Recently, Arabi et al. [15] and Sassi et al. [17] highlighted the existence of a great deviation between the results obtained by the different techniques. Arabi et al. [15] found that the deviations are more important in the cases of highly aerated slug flow. From a literature review, Webner et al. [18] explained that little attention has been paid to studying how measurement and calculation methods impact the determination of the slug frequency. This statement can be explained by the very limited number of studies where a comparison between the results obtained from different techniques and methods was carried out. Additionally, the great majority of experimental investigations on SF were carried out by using one technique or method. Each author discussed only the employed method. The presented statement explains the existing difficulty in capturing the state-of-the-art on measuring SF.

This review paper aims to fill this gap through a presentation and discussion of the existing knowledge on the different instruments, techniques, and methods developed and employed for measuring SF. The paper is structured in three levels following the flow diagram shown in Figure 2. At the first level, the two main categories of the instruments used for measuring will be discussed. Sections 2 and 3 are devoted to the visual observation/recording and flow parameters time series, respectively. From the video recording and time series signals, several methods were applied to extract SF. This part, summarized in Section 4, constitutes the second level. The third level is devoted to discussing the uncertainty in SF measurements (Section 5) and the results obtained from different instrumentation/techniques and methods (Section 6). Section 7 is committed to presenting the main conclusions as well as recommendations for future research.

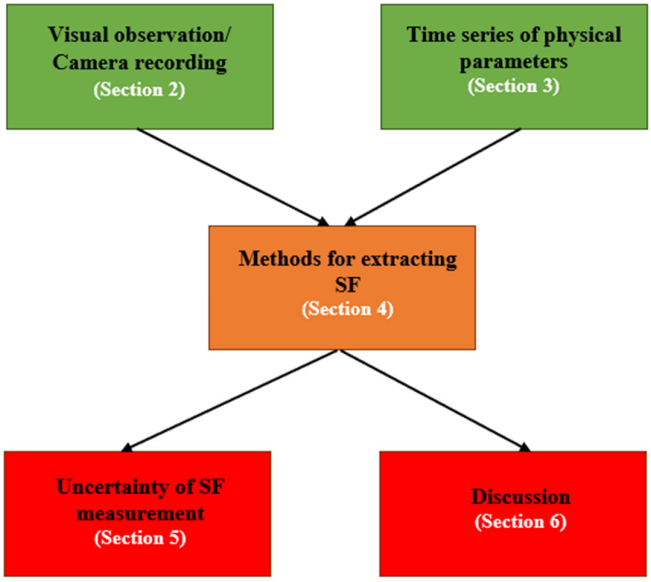

Figure 2. Schematic diagram of the content discussed in the present review.

2. Camera Video Recording

As explained in Section 1, the camera recordings were employed in early studies for SF measurement purposes. This technique is used up to today, especially with the development of high-speed cameras [19–26]. It has the advantage of not requiring calibration and validation [27]. In order to have high-quality video recordings, special attention has to be devoted to having a good illumination source. An example of an illumination system is given in Figure 3.

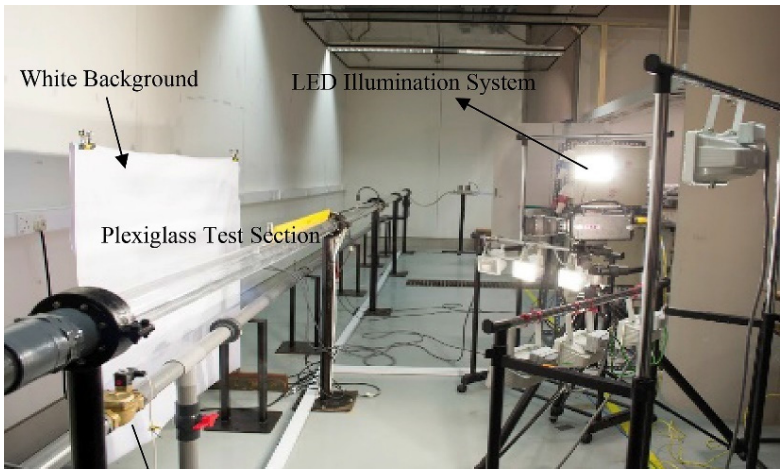

Figure 3. Example of illumination system used for camera video recordings used by Mohmmed et al. [22]. Reprinted from *International Journal of Pressure Vessels and Piping*, vol. 172, Abdalellah O. Mohmmed, Hussain H. Al-Kayiem, Mohammad S. Nasif, Rune W. Time, Effect of slug flow frequency on the mechanical stress behavior of pipelines, page 3, Copyright © 2019, with permission from Elsevier.

With the improvements of computer processing capacity, camera resolution, and framerate, several techniques have been used to extract quantitative flow data from video images [28]. The main efforts were performed to propose robust algorithms that are able to detect the elongated bubble/liquid slug interfaces, which deform and move continuously [29]. For instance, Sassi et al. [17] developed the line-scan image (LSI) method to extract the time series of interfaces from videos. First, videos were recorded using a fast camera with a resolution of 1 × 640 pixels in the axial and vertical directions, respectively, during a time of 75 s, which corresponds to a total of 240,000 frames for each run. Then, the

contrast of each image was enhanced through a pre-processing step involving background subtraction and histogram stretching. The line-scan image was obtained by positioning all the images sequentially, forming an image of 240,000 × 640 pixels. The noses and tails of both slug flow structures can be easily shown in the obtained line-scan image, as it appears in Figure 4a. Furthermore, a calculation of the mean intensity in the vertical axis was performed, which gives a time series of the mean intensity when the interface of elongated bubbles and liquid slugs can be easily identified (Figure 4b). A relatively similar technique was employed in Porter et al. [28].

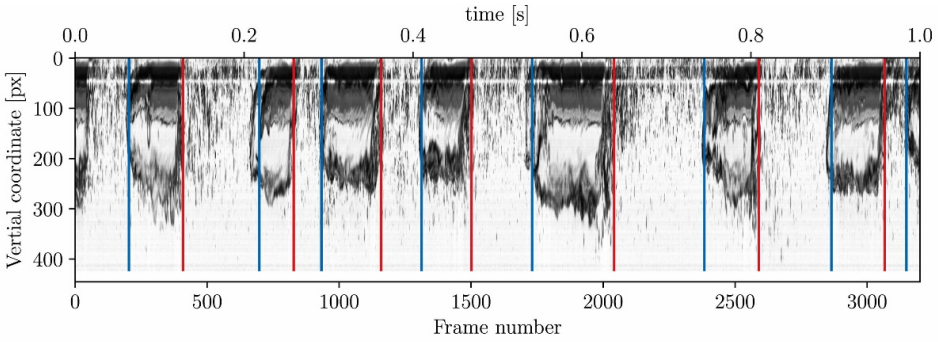

(a) Line-scan image with location of noses (blue) and tails (red lines) of Taylor bubbles.

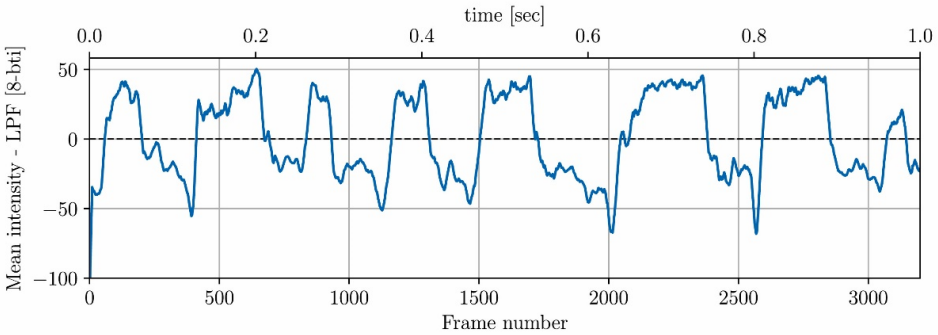

(b) Zero-mean intensity in vertical coordinate with low pass filter.

Figure 4. Elongated bubble location using LSI method (air–water, 30 mm ID, $\theta = 0°$, $V_{SL} = 1.5$ m/s and $V_{SG} = 0.58$ m/s). Reprinted from Sassi et al. [18]. Copyright © 2022, Paulo Sassi et al.

In the vertical and near-vertical configurations, the interface of the Taylor bubble is complicated to detect. Indeed, the liquid film surrounding the Taylor bubble can present a high aeration level. To overcome this constraint, Fadlalla et al. [29] applied simultaneously two video processing algorithms (adaptive thresholding (AT) and background subtraction (BS)) to video recordings for extracting void fraction time series. AR and BS are two algorithms of machine vision that allow, according to the authors, "*to interpret, process, and understand visual information from the environment*". The authors explained that the utilization of this combined method allowed them to use the advantage of each algorithm, permitting them to better capture both Taylor bubble/liquid slug and gas bubbles/liquid slug interfaces.

However, the direct/camera visualization technique has two main drawbacks: the use of transparent pipes, which implies its use only at a laboratory scale; and the difficulty to visualize the liquid slugs at high gas superficial or mixture velocities where the slugs become highly aerated due to complex phenomena, such as coalescence and the breakup of gas bubbles [30–35].

3. Time Series Signals of Physical Parameters

To overcome the weakness of the camera recording, explained in Section 2, several researchers have used and/or developed specific techniques to detect the passage of the

liquid slugs and elongated bubbles [36,37]. This can be achieved by collecting the temporal signals of parameters that are "sensitive" to the passage of liquid slugs and elongated bubble interfaces. Furthermore, the passage of liquid slugs and elongated bubbles induces important differences in the values of some physical parameters, as shown in Figure 5, with a void fraction time series. In addition, the obtained time series allows us to quantify the number of liquid slugs passing.

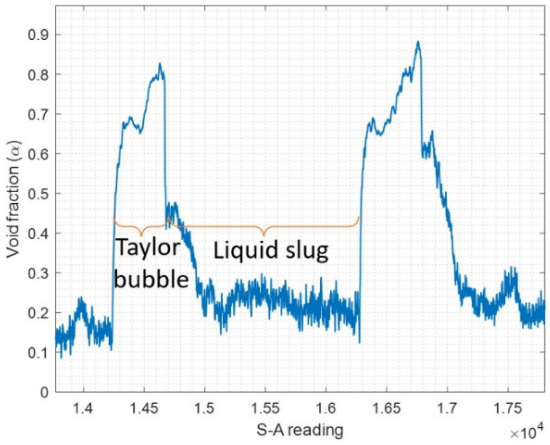

Figure 5. Example of void fraction time series collected by Maldonado et al. [34] using a capacitive wire-mesh sensor showing the region of Taylor bubble and liquid slug. Reprinted from *Experimental Thermal and Fluid Science*, vol. 151, Paul A. D. Maldonado, Carolina C. Rodrigues, Ernesto Mancilla, Eduardo N. dos Santos, Roberto da Fonseca Junior, Moises A. Marcelino Neto, Marco J. da Silva, Rigoberto E. M. Morales, Spatial distribution of void fraction in the liquid slug in vertical Gas-Liquid slug flow, page 5, Copyright © 2023, with permission from Elsevier.

3.1. Instrumentations

The different instrumentation employed to collect the different flow parameters sensitive to the passage of liquid slugs and elongated bubbles are summarized in Table 1.

Table 1. Summary of the different instrumentations used for the measurement of SF.

Physical Parameter	Instrumentation	References
-	Optical probe	[38–44]
	Laser sensor	[45]
	Non-invasive ultrasonic transducer	[46]
	Infrared ray detecting device	[47]
	Distributed acoustic sensing (DAS)	[8]
Liquid holdup/void fraction	Capacitance/capacitive sensor	[48–58]
	Conductance/conductivity probe	[59–65]
	Four-sensor conductivity probe	[66]
	Impedence void-meter	[67]
	Electrical capacitance tomography (ECT)	[68–72]
	Electrical resistance tomography (ERT)	[73,74]
	Gamma ray densitometer	[75–83]
	Wire-mesh sensor (WMS)	[84–87]
	Resistivity sensor	[88–92]
	Differential pressure transducer	[93]
	High-speed camera	[29]

Table 1. *Cont.*

Physical Parameter	Instrumentation	References
Absolute/gauge pressure	Absolute/gauge pressure transducer	[10,94–96]
Differential pressure	Differential pressure transducer	[15,97–100]
Liquid velocity	Ultrasound Doppler velocimetry (UDV)	[101,102]
	Particle image velocimetry (PIV)	[103]
	Laser Doppler velocimetry (LDV)	[104]
Gas velocity	Shadow size technique (SS)	[105]

Here, the instrumentation is classified according to the physical parameter associated with it. Images of some instrumentation indicated in Table 1 are depicted in Figure 6. As a reminder by Errigo et al. [106], some instrumentations can be invasive (requiring direct contact with the multiphase flow medium) or intrusive (requiring its location within the multiphase flow medium). Each instrument has its own advantages and weaknesses, and it is difficult to find one that combines the qualities of being inexpensive, non-intrusive, and offering a good resolution [107].

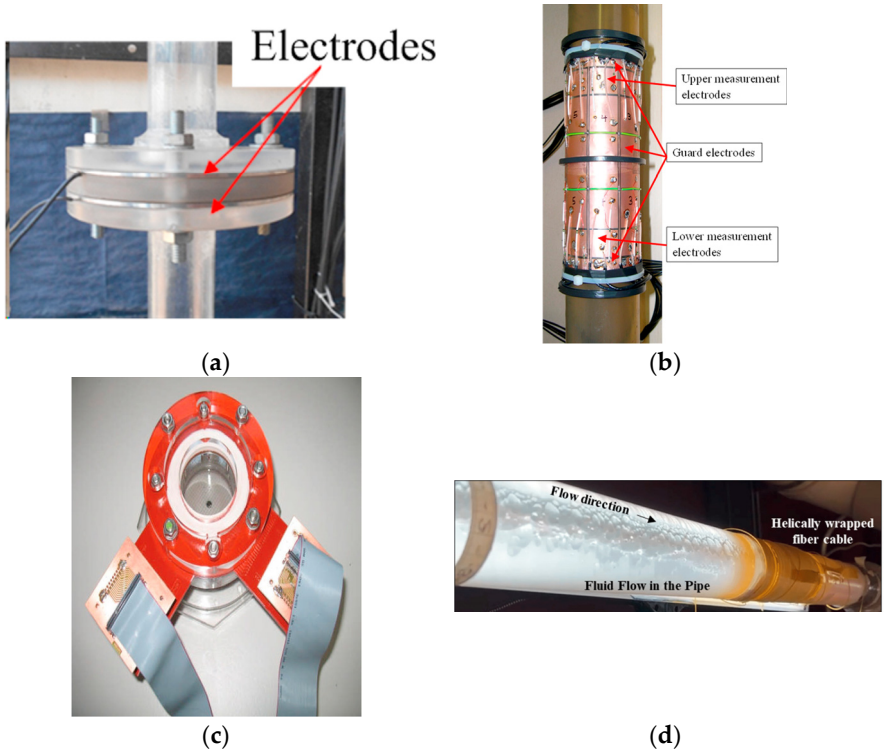

Figure 6. Examples of (**a**) conductance probe; (**b**) ECT; (**c**) WMS used in Zhao et al. [86] (Copyright ©2016, Zhao et al.); and (**d**) wrapped fiber cable of distributed acoustic sensing (DAS) used by Ali et al. [8] (Copyright ©2024, Ali et al.).

The optical probe technique is based on the difference in refractive indexes between gas and liquid phases [108]. Therefore, the optical probe can be used basically as a phase identifier for the gas–liquid mixture. Thus, the signals provided by this technique allow us to distinguish between liquid and gas phases. Note that the obtained signal does not necessarily represent the cross-sectional liquid holdup or void fraction. The same remark holds for the non-invasive ultrasonic transducer, laser sensor, and DAS.

The void fraction, or liquid holdup, is considered the most important parameter to characterize the gas–liquid two-phase flow [29]. This fact explains the popularity of using

this kind of signal for measuring SF as well as the great variety of developed instrumentations. Generally, this kind of instrumentation is based on the difference in conductivity or permittivity of the gas and liquid phases. The electrical conductivity is used in the case of conductive liquids, such as water, while the electrical capacitance is employed for non-conductive fluids, such as oil [58].

If the majority of the instrumentations, such as conductance and capacitance probes, give a global void fraction/liquid holdup (cross-sectional averaged), the techniques based on tomography (ECT, ERT, and WMS) and the four-sensor conductivity probe allow us to measure the void fraction/liquid holdup at different positions through cross-sectional pipe. The present review focuses only on the measurement of the slug frequency, and thus, no detailed information about these instrumentations is presented. The interested reader can find further information and deep discussions on the different instrumentations in Refs. [58,109–114]. Note that if the majority of the void fraction/liquid fraction measurements have been developed for laboratory scale utilization, several efforts have been carried out these recent years for extending their applicability to industrial scales [58,113–117]. As achievements, some tomographic techniques such as ERT, ECT, and WMS have reached TRL 7 to TRL 9 [113]. Yu et al. [93] used the pressure drop time series acquired between two points in a vertical pipe to extract the temporal signals of the void fraction. This was performed by subtraction of the calculated theoretically frictional pressure drop term from the total measured pressure drop to extract the gravitational pressure drop. The latter is directly related to the void fraction. Further details about this method can be found in Jia et al. [118]. It should be noted that this method can only be applied to vertical and inclined pipes. As mentioned in Section 2, the flow videos can also be used to extract the void fraction. The main weakness of this approach relies on the fact that the collected images give a 2D measurement, and thus, the third dimension is neglected [29]. Additionally, the accuracy of detecting correctly the bubble images is strongly influenced by the resolution of the imaging system and lighting conditions [29]. The pressure (absolute, gauge, differential) transducers are easy to use and are largely employed in industry. Further details about this technique are summarized in Ref. [119]. The techniques for measuring liquid and gas velocities are local methods. Furthermore, the measurement point location has to be chosen correctly for capturing the passage of the two intermittent structures. Due to the effect of gravity force on the elongated bubble shape (see, for instance, Figure 1), it is better to consider the measurement point near the upper wall and near the center of the pipe in the cases of horizontal and vertical pipes, respectively.

3.2. Objective Methods to Detect the Liquid Slugs and Elongated Bubble

The detection of the liquid slugs and the elongated bubbles from temporal signals is not always an easy task. Indeed, as explained in Section 2, the high aeration of the liquid slugs in the region of high values of gas or mixture velocity has as consequence that the slug liquid holdup does not reach important values when liquid slugs pass by. This induces a difficulty to discern between the traces left by the liquid slugs and the elongated bubbles. One also notes that due to the effect of the buoyancy in horizontal and inclined pipes, the gas distribution within liquid slugs is not homogenously distributed along the radial direction [18], and the shape of the gas/liquid interface can be strongly distorted [120]. This further complicates the detection of the liquid slugs. In horizontal and slightly inclined pipes, the occurrence of pseudo-slugs, roll waves, and/or waves in the zones of high gas superficial velocity and low liquid superficial velocity produces the apparition of additional peaks in the time series, inducing an overestimation of SF calculation, as shown in Figure 7. In vertical upward flow, the detection of the liquid slug nose/Taylor bubble tail interface is further complicated by the presence of wakes, produced by flow recirculation regions just behind the Taylor bubbles [5,121], and the presence of small bubbles surrounding the Taylor bubbles [29].

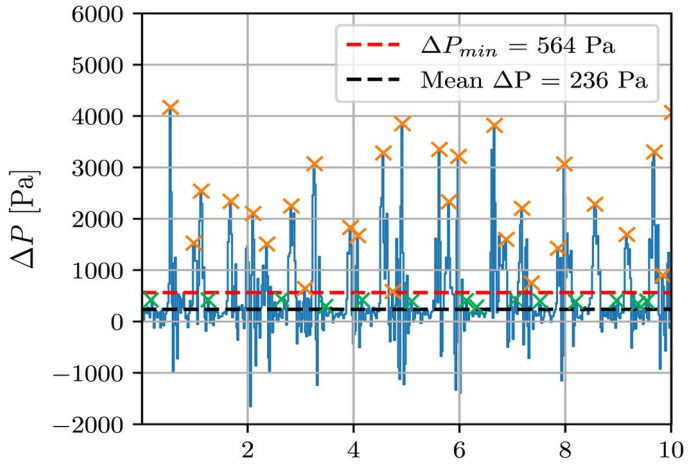

Figure 7. Example of pressure drop time series showing the peaks induced by the passage of liquid slugs (orange crosses) and by the presence of different kinds of flow structures (waves, roll waves or pseudo slugs) (green crosses). Copyright ©2022, Sassi et al. Note that the green crosses are added and not part of the original source.

Despite these problems, several authors [69,71,84] worked with these "raw" signals. With the liquid holdup or void fraction time series, other research groups preferred to use a critical value of these parameters to differentiate between the two structures. For horizontal pipe, Nydal [122] considered a threshold value (TV) of 0.7 of the liquid holdup for this instance. The values of liquid holdup greater and less than this critical value are considered the traces left by the liquid slugs and the elongated bubbles, respectively (Figure 8). Note that this critical value was also considered for vertical pipe [123] and annulus pipe [124]. As mentioned in Abdul Basith et al. [125], Manolis [126] used a critical value of 0.85 as the threshold value. All these studies were carried out with air–water or air–silicone oil mixtures. Okezue [80] selected 0.7 as the threshold value of liquid holdup for his experiments carried out with high-viscosity liquid–gas two-phase flow. Archibong-Eso [127] explained that the liquid holdup of the elongated bubble/liquid film structure for high viscosity two-phase flow can be higher than 0.7. By inspecting the time series for different liquid slugs, Schmelter et al. [128] concluded that it is not possible to have one universal threshold value. As a consequence, it has to be chosen carefully and individually for each time series [129]. On the other hand, Zhao et al. [68], Baba et al. [72,81], and Dong et al. [56] used the mean of the maximal and the minimal recorded liquid holdup values for each signal as TV. While Archibong-Eso et al. [130] used the mean of liquid holdup values for a time series as a threshold value. Note that the term threshold is also referred to as a cut and cut-off factor in some references [88,90].

If TV is used for liquid holdup and void fraction time series, Wilkens and Thomas [98] applied them for pressure drop time series to isolate the pictures left by the liquid slugs and those due to the presence of pseudo-slugs and waves. The threshold value is based on the calculation of the minimal value of pressure drop generated by the passage of one liquid slug given by Equation (1).

$$\Delta P_{one\ slug} = 2f\frac{L_{s,\ W\&T}\rho_s V_s^2}{D}, \tag{1}$$

where f, $L_{s,W\&T}$, ρ_S, V_S, and D are the Fanning friction factor, the considered liquid slug length, slug density, slug translational velocity and pipe diameter, respectively. The slug velocity is approximated by the mixture velocity (Equation (2)).

$$V_M = V_{SL} + V_{SG}, \tag{2}$$

The authors employed the formula of Drew et al. [131] to calculate the Fanning friction factor (Equation (3)).

$$f = 0.0014 + \frac{0.125}{Re_s^{0.32}}, \tag{3}$$

where Re_s is the Reynolds number of liquid slugs, calculated as follows:

$$Re_s = \frac{\rho_L D V_s}{L}, \tag{4}$$

where ρ_L and μ_L are the liquid density and viscosity, respectively.

The considered liquid slug length is given as follows:

$$L_{s,\,W\&T} = \begin{cases} L_{min}\ if\ L_{min} \leq L_{DP} \\ L_{DP}\ if\ L_{min} \geq L_{DP} \end{cases}, \tag{5}$$

where L_{min} and L_{DP} are the minimum length of a stable hydrodynamic slug and the differential pressure tap spacing, respectively. The former is calculated through Equation (6).

$$L_{min} = D(10\ V_{SL} + 5), \tag{6}$$

The W&T method was validated with video recording measurements. An average relative error of 5% was reported.

On the other hand, Ujang [132] used the translational velocity to discern between the liquid slugs from pseudo-slug/roll wave structures. She extracted the velocity of each structure visible in liquid holdup by dividing the distance between the two by the time lag, Δt_{slug} or Δt_{wave}, which is the time the peak front takes to travel between those probes. The SF was computed by considering only the peak that has a velocity greater than V_M. Indeed, the pseudo-slug and roll wave structures flow with a velocity lower than V_M.

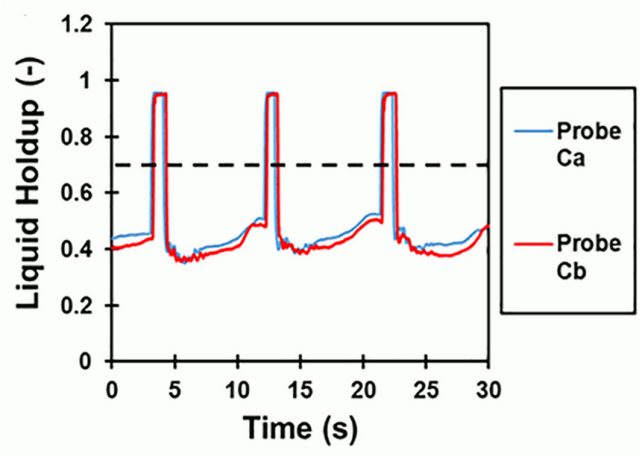

Figure 8. Experimental holdup time series with depiction of the threshold to detect the passage of liquid slugs. Reproduced from Eyo and Lao [124]. Reprinted from *AICHE Journal*, vol. 65, e16711, Edem N. Eyo, Liyun Lao, Slug flow characterization in horizontal annulus, page 5, Copyright © 2019 American Institute of Chemical Engineers, with permission from WILEY.

3.3. Signal Binarization Techniques

Some researchers preferred to binarize the obtained time series in order to obtain square signals with only two values: 0 and 1. This technique is notably used for extracting the liquid slug (L_s) and elongated bubble (L_{eb}) lengths. In his PhD thesis, Kouba [48] binarized the time series of liquid holdup using a threshold value. Each point of the time series that is superior to the threshold values becomes 1, otherwise, it is assigned a value of zero. The threshold value is chosen subjectively depending on the time series trace; i.e., for each signal (and thus for each experimental condition), a specific *TV* is selected. Examples

of the original signal (a) and binarization signals are given in Figure 9a. Losi et al. [54], Rosas et al. [89], Babakhani Dehkordi et al. [43], and Rodrigues et al. [87,90] employed this method. These works were carried out for horizontal and slightly horizontal pipes. Mi et al. [67] applied this technique for the case of vertical pipe, but there are no details about how the binarization was performed.

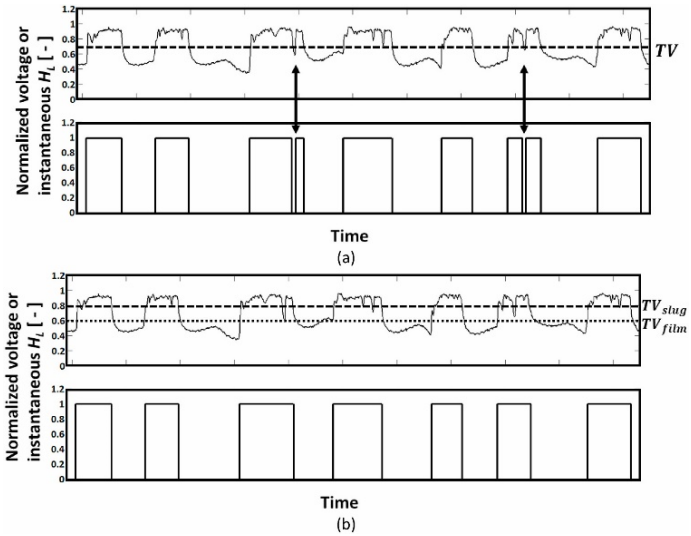

Figure 9. Threshold cut value applied to a normalized voltage or an instantaneous liquid holdup time series. (**a**) using a single threshold value (*TV*) and (**b**) using one threshold value for slug region (TV_{slug}) and the other for the film (TV_{film}). Reprinted from *Flow Measurement and Instrumentation*, vol. 79, Gabriel Soto-Cortes, Eduardo Pereyra, Cem Sarica, Carlos Torres, Auzan Soedarmo, Signal processing for slug flow analysis via a voltage or instantaneous liquid holdup time series, page 2, Copyright © 2021, with permission from Elsevier.

More recently, Naidek et al. [92] extracted the derivative of the time series. This allowed them to identify the fronts of the elongated bubbles and liquid slugs through the apparition of peaks in derivative time series. Then, the threshold value can be selected. On the other hand, dos Santos et al. [58] used the probability density function (PDF) for each time series to select the threshold value. Considering that the PDF obtained from void fraction/liquid holdup time series in the case of intermittent flow has a bimodal shape, the authors considered the value of void fraction corresponding to the lower value of PDF between the two peaks as the threshold value.

As discussed and analyzed by Soto-Cortès et al. [133], the use of a threshold value to isolate the two intermittent structures has the disadvantage of considering the waves and pseudo-slugs as slug flow, as well as one slug pulse can be considered as two separated liquid slugs (see, for instance, the black arrows in Figure 9a). In addition, there is no consensus about the threshold value, and one has to check the effect of the value on capturing the slug unit [43] or by applying the binarization technique together with flow image analysis [134]. To overcome these limits, Al-Safran [135] used two threshold values as depicted in Figure 9b. The higher and lower threshold values (TV_{slug} and TV_{film}, respectively) are used to detect the liquid slugs and elongated bubbles, respectively. Meanwhile, the choice of two values of *TVs* remains subjective. Additionally, the cases when the liquid holdup values are between the two threshold values are confusing [136]. Based on the critical analysis of these two techniques, Soto-Cortès et al. [133,137] proposed a new procedure when cut threshold values are calculated using a statistical algorithm, giving it the advantage of being objective. The method was validated notably through SF.

According to the literature review presented here, the techniques for detecting the passage of elongated bubbles and liquid slugs are mostly developed for horizontal and

slightly horizontal pipes. This can be explained by the fact that the slug frequency was mainly studied for these pipe inclinations.

4. Methods for Calculating SF

From the recording videos or from signal time series, several methods were proposed to calculate the slug frequency. These can be classified into two direct categories: counting method and power spectral density (PSD).

4.1. Counting Method

From different types of time series as well as video recordings provided from cameras, the SF can be estimated through the counting method. The mean SF ($\overline{f_s}$) is the number of peaks generated by the liquid slugs passage (N) over the time series duration (T) as follows:

$$\overline{f_s} = \frac{N}{\Delta T}, \tag{7}$$

In addition to this intuitive method, SF can also be computed for each slug (f_s) through the time between two consecutive slugs (ΔT_s) [38,138]. In this case, the nose or the tail of the liquid slugs (or elongated bubble) are chosen as a reference point.

Similarly, some authors extracted from time series the translational or residence time of the slug unit (T_{su}) given by Equation (8), which is the time needed for a slug unit to pass through a certain cross-section [5,29,85,87,90]. Thus, it is the sum of the translational times of the elongated bubble (T_{eb}) and of the liquid slug (T_{ls}), as depicted in Figure 10.

$$f_s = \frac{1}{T_{su}} = \frac{1}{T_{eb} + T_{ls}}, \tag{8}$$

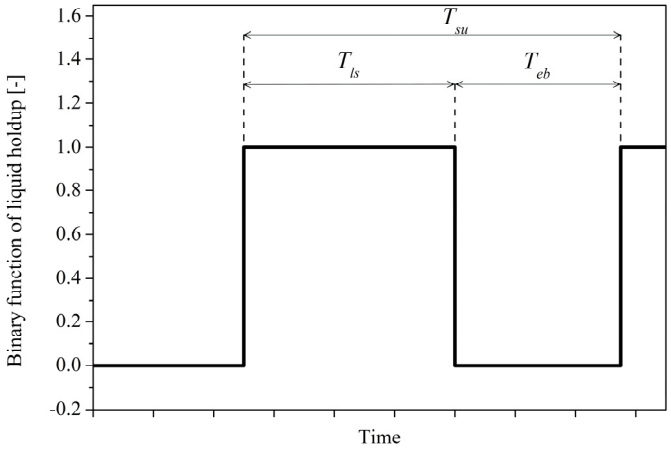

Figure 10. Example of binarized liquid holdup signals showing the translational times of liquid slug (T_{ls}) and elongated bubble (T_{eb}).

On the other hand, do Ameral et al. [19] computed SF from the elongated bubble translational velocity (V_{TB}) and the length of slug unit (L_{su}) (Equation (9)). The latter is the sum of lengths of liquid slug (L_{ls}) and elongated bubble (L_{eb}).

$$f_s = \frac{V_T}{L_{su}}, \tag{9}$$

The results of SF given by Equations (8) and (9) are for each slug unit or liquid slug. The mean SF values are calculated by averaging the values collected for the N slug unit as follows:

$$\overline{f_s} = \frac{1}{N}\sum_{i=1}^{N} f_s, \tag{10}$$

The classical counting method (Equation (7)) gives only the mean value, while the estimation of SF from the calculation of the residence time allows to know the SF of each passing slug. Furthermore, this method also allows to extract the statistical distribution of SF. Thus, a statistical study can be carried out. On the other hand, the classical counting method has the advantage of being easy to apply.

4.2. Power Spectral Density (PSD)

SF can be estimated from the frequency spectrum obtained using the power spectral density. This mathematical tool allows detecting the frequencies present in a time series and assigning them to various physical phenomena in a system [139]. The PSD can be obtained by applying the Fast Fourier Transform (FFT) algorithm to the autocorrelation of a time series [7,15,71,123,140]. An example of PSD is given in Figure 11. The frequency corresponding to the higher PSD value is termed the dominant frequency, while the other peaks result from the presence of harmonic frequencies [15,51]. Traditionally, the dominant frequency is usually associated with SF [15,26,51,75,141,142]. Schmelter et al. [129] explained that computing PSD from the Welch method gives more robust results than a pure FFT. This is due to the additional smoothing performed by the Welch method, which allows better highlighting the desired phenomenon (SF in this case) [143].

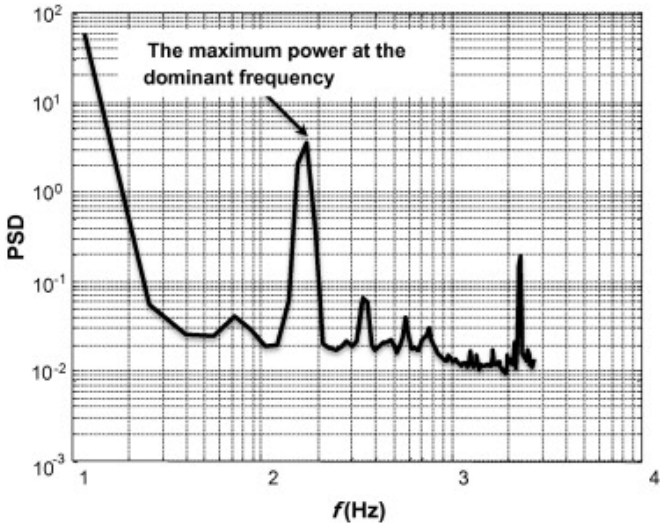

Figure 11. Example of frequency spectrum obtained by applying PSD to the void fraction time series. Taken from [141]. Reprinted from *International Journal of Multiphase Flow*, vol. 37 (8), Wael H. Ahmed, Experimental investigation of air–oil slug flow using capacitance probes, hot-film anemometer, and image processing, page 886, Copyright © 2011, with permission from Elsevier.

5. Uncertainty of SF Measurement

There are few works where the uncertainties in the measurement of SF were estimated and given. Kesana et al. [144] mentioned that the uncertainty associated with SF arises from the number of liquid slugs passing by the sensor during the acquisition time. The uncertainty was evaluated from the standard deviation calculated using measurements obtained by subdividing the signals into segments. Bertola and Cafaro [40] found that PSD gives higher values of standard deviation compared with the counting method. On the other hand, Bressani and Mazza [134] explained that the uncertainties associated with SF, which were estimated from the residence time, are due to the bubble nose velocity, the resident contact time, and the threshold value chosen for the binarization. They estimated the uncertainty to be about 1.2%. Soedarmo [145] calculated the uncertainty of SF by the ratio of 2 over the acquisition time duration. For the cases where the structure frequencies were estimated from two probes placed at different positions, Soedarmo [145] added the ratio of the difference between the results given by the two probes used to the acquisition

time duration. For the slug frequency obtained from the high-speed camera computed using Equation (9), Fadlalla et al. [29] estimated its uncertainty by evaluating the error in the measurement of the time and the length of the slug using the recorded images.

6. Discussions

The present review has highlighted a great number of developed instrumentations, techniques, and methods, yet there are few works where these are compared. In Table 2, we summarize the findings reported by the studies comparing different techniques. In general, a good agreement is observed; meanwhile, some important deviations were reported by applying PSD and the counting method (with or without signal binarization) to the liquid holdup/void fraction time series [84,93,145].

Table 2. Summary of the findings reported obtained by comparing the results obtained by the different instrumentation, techniques and methods.

Ref.	Fluids and Pipe Geometry Used	Techniques Used	Findings
Gregory and Scott [10]	Air–water, 19.05 mm ID, and $\theta = 0^\circ$	Manually counting of the passed slug, and pressure time series (counting)	"Good agreement" was reported according to the authors
Odozi [78]	Air–water–oil, 77.92 mm ID, and, $\theta = 0^\circ$	Video camera (counting) and liquid holdup time series (counting)	"Good agreement" was reported according to the authors
Kaji et al. [84]	Air–water, 52.3, and $\theta = 90^\circ$	Void fraction time series (counting and PSD)	The counting methods slightly overestimates the results with a difference ranging from −20% to +50%.
Kesana et al. [145]	Air–water and air–water+carboxy methyl cellulose (CMC), 76.2 mm ID, and $\theta = 0^\circ$	Void fraction time series (counting and PSD)	The counting method slightly underestimates the results obtained by PSD with a difference ranging between −30% and +20%
Zhao et al. [68]	Air–oil, 26 and 74 mm ID, and $\theta = 0^\circ$	Liquid holdup time series (counting with a binarized signal and PSD)	"Consistent values" were obtained according to the authors
Abdulkadir et al. [123]	Air–silicone oil, 67 mm ID, and $\theta = 90^\circ$	Void fraction time series (counting with a threshold value of 0.3 and PSD)	"Reasonably good agreement" was reported according to the authors
Jaeger et al. [96]	Air–water, 94 mm ID, and $\theta = 90^\circ$	Camera video (counting) and pressure time series (counting and PSD)	"Good agreement" was reported according to the authors
Akhlaghi et al. [146]	Air–water, 44 mm ID, and, $\theta = 0^\circ$	Video (counting) and pressure time series (PSD)	The difference in the results obtained by both methods are in the range of ±5%.
Arabi et al. [15]	Air–water, 30 mm ID, and $\theta = 0^\circ$	Pressure drop time series (PSD, counting and W&T method)	The W&T method overtimes the results of PSD with a deviation between −20% and +700%. The counting method largely overestimates the results of PSD with a deviation ranging from +15% to +900%.
Sassi et al. [17]	Air–water, 30 mm ID, and $\theta = 0^\circ$	Video recordings (LSI) and pressure drop time series (PSD, counting and W&T method)	The W&T method and PSD slightly overestimate the results compared to those obtained by LSI.
Yu et al. [93]	Air–water, 80 mm ID, and $\theta = 90^\circ$	Void fraction time series (counting and PSD)	The PSD slightly overestimates the results with a difference ranging from −20% to +30%.
Dos Santos et al. [58]	Air–oil, 50.8 mm ID, and $\theta = 0^\circ$	Void fraction time series (counting in a binarized signal and PSD)	"Agreement" between the results obtained by the two method was reported by the authors

Arabi et al. [15] compared the results obtained by three methods based on the pressure drop time series, which include the counting method (when all the peaks are counted), the W&T methods, and PSD. The authors recommended using PSD. Indeed, according to their analysis, the W&T method is not applicable when the liquid slugs are strongly aerated and when several liquid slugs are present simultaneously in the space between the pressure taps. On the other hand, the counting method largely overestimated the results compared to the two remaining methods.

Sassi et al. [17] extended the work of Arabi et al. [15] by comparing the results obtained through the pressure drop time series (using the W&T method and PSD) with the results obtained using LSI (through the estimation of residence times and PSD applied to the mean intensity signal of LSI). The results obtained from residence times extracted from the mean intensity signal of LSI were considered by the authors as the references ones. It was found that the W&T method tends to overestimate the results for low superficial liquid ranges. Note that the authors employed two different lengths of space between the pressure taps for the W&T method (L_{DP} = 25 cm and 50 cm). Analyzing the presented results by Sassi et al. [17] (depicted in Figure 12), one can observe that better results were obtained with smaller pressure tap distances, which confirms the fact that the precision of this method decreases when several liquid slugs are simultaneously present in the space between the pressure taps, as stated in Arabi et al. [15]. Concerning the results obtained from PSD, Sassi et al. [17] reported that the application of this method to both kinds of signal give, in general, good SF results. Better results were obtained by the temporal signal of the mean intensity signal of LSI.

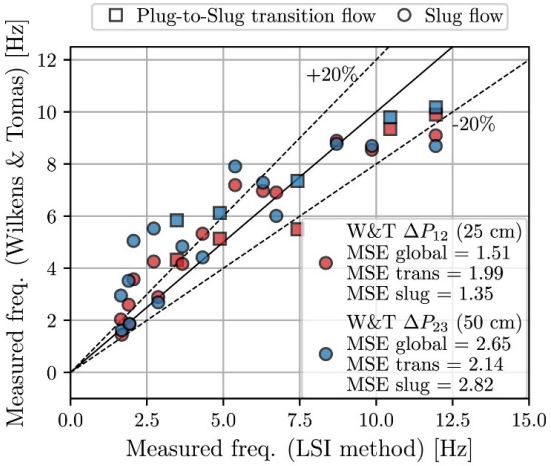

Figure 12. Comparison between the measured slug frequency using W&M method applied for two pressure tap distances and LSI method obtained by Sassi et al. [17]. Copyright © 2022, Paulo Sassi et al.

On the other hand, Sassi et al. [17] pointed out also the main problem of PSD. Indeed, in some cases, the frequency spectrum exhibits several peaks of the same power, inducing difficulty to determine the main frequency. This problem was previously pointed out by Hernandez-Perez et al. [51], Lin et al. [100], and Akhlaghi et al. [146]. This is due to the non-periodic standard function nature of SF and the stochastic nature of the slug flow [147]. The fact that the actual FFT algorithms still present some limitations [148] can be a reason to consider the results given by the PSD as just an estimation of SF. The PSD also has the problem of being dependent on the filtering technique used [75]. The application of low pass filters to obtain the PSD has to be performed with care to not hide the natural slug frequency [17]. Bertola and Cafaro [40] found that PSD and counting methods gave similar results for low liquid and gas superficial velocities. Higher liquid and gas superficial velocities conditions induced the presence of two or three dominant frequencies in the PSD spectrum. In this case, any dominant frequency matched with the value given by the

counting method. The latter observation can also be shown with the data presented by Schmelter et al. [128].

Some studies compared the results obtained using different instrumentations collecting time series of different physical parameters. Hernandez-Perez [149] reported that measurements of SF obtained using the pressure drop time series are lower than those obtained using the liquid holdup time series. The author explained that the distance between the pressure drop taps can be longer or shorter than the lengths of the slug structures. Thus, the pressure drop time series cannot detect some fluctuations. The same observation was reported in Azzopardi et al. [150] by comparing the void fraction and pressure drop time series. One should note that the experiments of Azzopardi et al. [150] were carried out for zero liquid superficial velocity, which corresponds to batch bubble column reactor conditions [151–154]. By comparing the signature of the time series of liquid holdup and absolute pressure, Woods et al. [155] explained that the signals provided by the latter instrumentation detect better the passage of liquid slugs in the conditions of high gas superficial velocities. On the other hand, Luo et al. [156] explained that the passage of liquid slugs is better "captured" with differential pressure transducers than absolute pressure transducers. Indeed, the peaks are more apparent with this kind of signal. This is due to the fact that the pressure drop time series filters out the fluctuations originating from outside the space between the two pressure taps [157]. To the authors' best knowledge, there are no works where the measurements of slug frequency obtained by different techniques measuring void fraction/liquid holdup time series have been compared.

Regarding the threshold values for the binarization of the signal, Rodrigues et al. [87] studied the influence of the particular threshold values selected from the obtained results and concluded that with a maximum relative deviation of 2.24%, the threshold value has not a great influence on the determination of SF.

7. Conclusions and Recommendations for Future Works

SF is an important parameter for characterizing the intermittent two-phase flow. This parameter has been mainly studied experimentally, which implies the importance of correctly measuring it. In this paper, we presented a review of the different instrumentations, techniques, and methods that have been developed/used for this purpose.

Currently, several methods exist to extract SF from the inputs given by the videos or time series signals of several physical parameters. The camera recording remains the most reliable one. However, it can be used only at the laboratory scale. The estimation of SF from the residence time gives the advantage of extracting the distribution function, which is very useful for statistical characterization of SF. The PSD has the advantage of being easy to use and implement. Meanwhile, several peaks can appear for some cases, complicating the estimation of SF.

This review highlights that despite the efforts achieved, there is no complete and reliable instrumentation/technique/method able to measure SF for a great range of experiments. Therefore, the recourse to the high-speed camera, and thus, to transparent pipe, remains the most reliable tool, notably for the validation purposes.

Based on the synthesized state-of-the-art, the authors strongly recommend future studies perform the following:

- Pursue efforts for developing and optimizing the measurement techniques and methods. To achieve this goal, improvements of the techniques for the selection of the threshold values for distinct between the traces left by elongated bubbles and liquid slugs are required. The approach proposed recently by Soto-Cortès et al. [133,137] seems to be very promising, and additional validations, notably for different oil viscosities and pipe inclinations, have to be carried out.
- Extend the applicability of the instrumentation and methods to industrial/field scales by increasing the TRL. The conceptualization of transducers that are robust, easy to maintain, and able to work in harsh conditions (high temperature and pressure, occurrence of importance change in the operating conditions, and presence of complex

and abrasive fluids), as well as employing fast processors are the greatest challenges that have to be faced.
- Carry out more studies on vertical and inclined pipes.
- Encourage further comparison between the results obtained from different instrumentation techniques.
- Continue research on the most appropriate FFT algorithms for SF.
- Estimate of uncertainties associated with the measurement of SF.

Author Contributions: Conceptualization, R.L.H., A.A. and Y.S.; methodology, A.A.; writing—original draft preparation, R.L.H. and A.A.; writing—review and editing, Y.S. and J.P.; visualization, A.A.; supervision, Y.S.; project administration, Y.S. and J.P.; funding acquisition, Y.S. and J.P. All authors have read and agreed to the published version of the manuscript.

Funding: This work was supported through the projects PID2020-113303GB-C21 and PID2023-146648NB-C21, funded by Ministerio de Ciencia e Innovación (MCIN) and Agencia Estatal de Investigación (AEI), and by project 2021SGR00732 from the Departament de Recerca i Universitats de la Generalitat de Catalunya, as well as from the European Union's Horizon 2020 research and innovation program under the Marie Skłodowska-Curie grant agreement No. 713679 and No. 945413, through the Martı Franques COFUND Doctoral Programme. AA has received funding from the postdoctoral fellowships programme Beatriu de Pinós (2021 BP 00052), funded by the Secretary of Universities and Research (Government of Catalonia) and by the Horizon 2020 Programme of Research and Innovation of the European Union under the Marie Skłodowska-Curie grant agreement No. 801370.

Acknowledgments: AA would especially like to thank Youcef Zenati for all valuable discussions.

Conflicts of Interest: The authors declare no conflicts of interest.

Abbreviations

AT	Adaptive thresholding
BS	Background subtraction
CMC	Carboxy methyl cellulose
DAS	Distributed acoustic sensing
ECT	Electrical capacitance tomography
ERT	Electrical resistance tomography
FFT	Fast Fourier transform
FIV	Flow-induced vibration
LDV	Laser doppler velocimetry
LSI	Line-scan Image
PIV	Particle image velocimetry
PDF	Probability density function
PSD	Power spectral density
SF	Slug frequency
TRL	Technological readiness level
UDV	Ultrasound doppler velocimetry
W&T	Wilkens and Thomas
WMS	Wire-mesh sensor

Nomenclature

D	Pipe diameter	[m]
f	Fanning friction factor	[-]
f_s	Slug frequency	[s^{-1}]
$\overline{f_s}$	Mean slug frequency	[s^{-1}]
L_{DP}	Differential pressure tap spacing	[m]
L_{eb}	Elongated bubble length	[m]
L_{ls}	Liquid slug length	[m]
L_{su}	Slug unit length	[m]
$L_{s,\,min}$	Minimum length of a stable hydrodynamic slug	[m]
$L_{s,\,W\&T}$	Considered slug length in the Wilkens and method	[m]
N	Number of liquid slugs	[-]

Re_s	Slug Reynolds number	[-]
TV	Threshold value	[-]
TV_{film}	Threshold value for liquid film region	[-]
TV_{slug}	Threshold value for liquid slug region	[-]
T_{eb}	Translational time of the elongated bubble	[s]
T_s	Translational time of the liquid slug	[s]
T_{su}	Translational time of the slug unit	[s]
V_M	Mixture velocity	[m.s^{-1}]
V_s	Slug velocity	[m.s^{-1}]
V_T	Elongated bubble translational velocity	[m.s^{-1}]
V_{SG}	Gas superficial velocity	[m.s^{-1}]
V_{SL}	Liquid superficial velocity	[m.s^{-1}]
Greek letters		
ΔP	Pressure drop	[Pa]
$\Delta P_{one\ slug}$	Pressure drop generated by one liquid slug	[Pa]
ΔT	Time duration	[s]
ΔT_{slug}	Time lag between two consecutive slugs	[s]
ΔT_{wave}	Time lag between two consecutive waves	[s]
θ	Pipe inclination	[°]
μ_L	Liquid viscosity	[Pa.s]
ρ_L	Liquid density	[kg.m^{-3}]
ρ_s	Slug density	[kg.m^{-3}]

References

1. Ali, A.A.; Abdul-Majeed, G.H.; Al-Sarkhi, A. Review of Multiphase Flow Models in the Petroleum Engineering: Classifications, Simulator Types, and Applications. *Arab. J. Sci. Eng.* **2024**, 1–44. [CrossRef]
2. Arseniev, D.; Malykhina, G.; Kratirov, D. Wavelet Cross-Correlation Signal Processing for Two-Phase Flow Control System in Oil Well Production. *Processes* **2024**, *12*, 1479. [CrossRef]
3. Ma, X.; Gu, Z.; Ni, D.; Li, C.; Zhang, W.; Zhang, F.; Tian, M. Experimental Study on Gas–Liquid Two-Phase Flow Upstream and Downstream of U-Bends. *Processes* **2024**, *12*, 277. [CrossRef]
4. Liang, X.; Wang, S.; Shen, W. Analysis of Bubble-Flow Characteristics in Scavenge Pipe and Establishment of a Flow-Prediction Model. *Processes* **2024**, *12*, 1364. [CrossRef]
5. Holagh, S.G.; Ahmed, W.H. Critical review of vertical gas-liquid slug flow: An insight to better understand flow hydrodynamics' effect on heat and mass transfer characteristics. *Int. J. Heat Mass Transf.* **2024**, *225*, 125422. [CrossRef]
6. Colombo, M.; De Santis, A.; Hanson, B.C.; Fairweather, M. Prediction of horizontal gas–liquid segregated flow regimes with an all flow regime multifluid model. *Processes* **2022**, *10*, 920. [CrossRef]
7. Wu, B.; Firouzi, M.; Mitchell, T.; Rufford, T.E.; Leonardi, C.; Towler, B. A critical review of flow maps for gas-liquid flows in vertical pipes and annuli. *Chem. Eng. J.* **2017**, *326*, 350–377. [CrossRef]
8. Cazarez-Candia, O.; Benítez-Centeno, O. Comprehensive experimental study of liquid-slug length and Taylor-bubble velocity in slug flow. *Flow Meas. Instrum.* **2020**, *72*, 101697. [CrossRef]
9. Hubbard, M.G. *An Analysis of Horizontal Gas-Liquid Slug Flow*; University of Houston: Houston, TX, USA, 1965.
10. Gregory, G.A.; Scott, D.S. Correlation of liquid slug velocity and frequency in horizontal cocurrent gas-liquid slug flow. *AIChE J.* **1969**, *15*, 933–935. [CrossRef]
11. Arabi, A.; Höhn, R.L.; Pallares, J.; Stiriba, Y. Practical aspects of multiphase slug frequency: An overview. *Can. J. Chem. Eng.* **2024**, *in press*. [CrossRef]
12. Al-Safran, E.M. Probabilistic modeling of slug frequency in gas/liquid pipe flow using Poisson probability theory. In Proceedings of the BHR North American Conference on Multiphase Production Technology, Banff, AB, Canada, 20–22 June 2012; BHR: Bedford, UK, 2012; p. BHR-2012-A024.
13. Zhu, H.; Tang, T.; Li, Q. Flow-Induced Vibration of a Reversed U-Shaped Jumper Conveying Oil-Gas Two-Phase Flow. *Processes* **2023**, *11*, 1134. [CrossRef]
14. Ali, S.; Jin, G.; Fan, Y. Characterization of Gas–Liquid Two-Phase Slug Flow Using Distributed Acoustic Sensing in Horizontal Pipes. *Sensors* **2024**, *24*, 3402. [CrossRef] [PubMed]
15. Arabi, A.; Salhi, Y.; Zenati, Y.; Si-Ahmed, E.; Legrand, J. On gas-liquid intermittent flow in a horizontal pipe: Influence of sub-regime on slug frequency. *Chem. Eng. Sci.* **2020**, *211*, 115251. [CrossRef]
16. Hansen, L.S.; Pedersen, S.; Durdevic, P. Multi-phase flow metering in offshore oil and gas transportation pipelines: Trends and perspectives. *Sensors* **2019**, *19*, 2184. [CrossRef]
17. Sassi, P.; Fernandez, G.; Stiriba, Y.; Pallares, J. Effect of solid particles on the slug frequency, bubble velocity and bubble length of intermittent gas–liquid two-phase flows in horizontal pipelines. *Int. J. Multiph. Flow* **2022**, *149*, 103985. [CrossRef]

18. Webner, F.; Polansky, J.; Knotek, S.; Schmelter, S. Sensitivity analysis of threshold parameters in slug detection algorithms. *Int. J. Multiph. Flow* **2023**, *158*, 104278. [CrossRef]
19. Amaral, C.D.; Alves, R.; da Silva, M.; Arruda, L.; Dorini, L.; Morales, R.; Pipa, D. Image processing techniques for high-speed videometry in horizontal two-phase slug flows. *Flow Meas. Instrum.* **2013**, *33*, 257–264. [CrossRef]
20. Thaker, J.; Banerjee, J. Characterization of two-phase slug flow sub-regimes using flow visualization. *J. Pet. Sci. Eng.* **2015**, *135*, 561–576. [CrossRef]
21. Al-Kayiem, H.H.; Mohmmed, A.O.; Al-Hashimy, Z.I.; Time, R.W. Statistical assessment of experimental observation on the slug body length and slug translational velocity in a horizontal pipe. *Int. J. Heat Mass Transf.* **2017**, *105*, 252–260. [CrossRef]
22. Mohmmed, A.O.; Al-Kayiem, H.H.; Nasif, M.S.; Time, R.W. Effect of slug flow frequency on the mechanical stress behavior of pipelines. *Int. J. Press. Vessel. Pip.* **2019**, *172*, 1–9. [CrossRef]
23. Liu, A.; Cheng, L.; Yan, C.; Gu, H.; Meng, Z. Experimental study on length, liquid film thickness and pressure drop of slug flow in horizontal narrow rectangular channel. *Chem. Eng. Res. Des.* **2022**, *182*, 502–516. [CrossRef]
24. Doucette, A.; Holagh, S.G.; Ahmed, W.H. Experimental evaluation of airlift pumps' thermal and mass transfer capabilities. *Exp. Therm. Fluid Sci.* **2024**, *154*, 111174. [CrossRef]
25. Alegría, L.F.; Ortiz-Vidal, L.E.; Álvarez-Pacheco, C.; Bolivar, J.E.; Rodriguez, O.M. Influence of a restriction on flow patterns, void fraction, and pressure drop in gas–liquid pipe flow. *Exp. Therm. Fluid Sci.* **2024**, *155*, 111180. [CrossRef]
26. Huang, B.; Xu, Q.; Cao, Y.; Yu, H.; Li, Y.; Chang, Y.; Guo, L. Investigation on intermittent flow characteristics in horizontal pipe by visualization measurement method. *Experim. Thermal Fluid Sci.* **2024**, in press. [CrossRef]
27. RMadhumitha, R.; Balachandar, C.; Venkatesan, M. Flow regime identification using fuzzy and neuro-fuzzy inference applied on differential pressure sensor. *Flow Meas. Instrum.* **2023**, *94*, 102474. [CrossRef]
28. Porter, K.; Pereyra, E.; Mesa, J.; Sarica, C. Experimental investigation of induced vibrations in horizontal Gas-Liquid flow. *Exp. Therm. Fluid Sci.* **2023**, *149*, 111015. [CrossRef]
29. Fadlalla, D.; Holagh, S.G.; Ahmed, W.H.; Weales, D.; Moussa, M. Machine Vision Algorithms for Characterizing Gas-Liquid Slug Flows in Vertical Pipes. *Flow Meas. Instrum.* **2024**, *99*, 102671. [CrossRef]
30. Gregory, G.; Nicholson, M.; Aziz, K. Correlation of the liquid volume fraction in the slug for horizontal gas-liquid slug flow. *Int. J. Multiph. Flow* **1978**, *4*, 33–39. [CrossRef]
31. Abdul-Majeed, G.H.; Firouzi, M. The suitability of the dimensionless terms used in correlating slug liquid holdup with flow parameters in viscous two-phase flows. *Int. Commun. Heat Mass Transf.* **2019**, *108*, 104323. [CrossRef]
32. Abdul-Majeed, G.H.; Kadhim, F.; Almahdawi, F.H.; Al-Dunainawi, Y.; Arabi, A.; Al-Azzawi, W.K. Application of artificial neural network to predict slug liquid holdup. *Int. J. Multiph. Flow* **2022**, *150*, 104004. [CrossRef]
33. Thaker, J.; Banerjee, J. Influence of intermittent flow sub-patterns on erosion-corrosion in horizontal pipe. *J. Pet. Sci. Eng.* **2016**, *145*, 298–320. [CrossRef]
34. Maldonado, P.A.D.; Rodrigues, C.C.; Mancilla, E.; dos Santos, E.N.; Junior, R.d.F.; Neto, M.A.M.; da Silva, M.J.; Morales, R.E.M. Spatial distribution of void fraction in the liquid slug in vertical Gas-liquid slug flow. *Exp. Therm. Fluid Sci.* **2024**, *151*, 111093. [CrossRef]
35. Arabi, A.; Zenati, Y.; Legrand, J.; Si-Ahmed, E.-K. Sub-regimes of horizontal gas–liquid intermittent flow: State-of-the-art and future challenges. *Exp. Therm. Fluid Sci.* **2024**, *160*, 111281. [CrossRef]
36. Falcone, G.; Hewitt, G.F.; Alimonti, C.; Harrison, B. Multiphase Flow Metering: Current Trends and Future Developments. *J. Pet. Technol.* **2002**, *54*, 77–84. [CrossRef]
37. Arabi, A. Contribution à l'étude du Comportement d'un Écoulement Diphasique dans une Conduite en Présence d'une Singularité. Ph.D. Thesis, USTHB, Algiers, Algeria, 2019.
38. Ferré, D. Ecoulements Diphasiques à poches en conduite horizontale. *La Houille Blanche* **1979**, *34*, 113–142. [CrossRef]
39. Kvernvold, O.; Vindøy, V.; Søntvedt, T.; Saasen, A.; Selmer-Olsen, S. Velocity distribution in horizontal slug flow. *Int. J. Multiph. Flow* **1984**, *10*, 441–457. [CrossRef]
40. Bertola, V.; Cafaro, E. On the measurement of slug frequency in the horizontal gas-liquid flow. In Proceedings of the 15th AIAA Computational Fluid Dynamics Conference, Anaheim, CA, USA, 11–14 June 2001; p. 3035.
41. van Hout, R.; Shemer, L.; Barnea, D. Evolution of hydrodynamic and statistical parameters of gas–liquid slug flow along inclined pipes. *Chem. Eng. Sci.* **2003**, *58*, 115–133. [CrossRef]
42. Salhi, Y. Contribution théorique et expérimentale à l'étude des phénomènes de Transition d'un écoulement Stratifié à l'écoulement Poche/Bouchon dans une Conduite Horizontale en Présence de Singularité. Ph.D. Thesis, USTHB, Algiers, Algeria, 2010.
43. Dehkordi, P.B.; Colombo, L.; Mohammadian, E.; Arnone, D.; Azdarpour, A.; Sotgia, G. Study of viscous oil-water-gas slug flow in a horizontal pipe. *J. Pet. Sci. Eng.* **2019**, *178*, 1–13. [CrossRef]
44. Wang, T.; Gui, M.; Zhang, T.; Bi, Q.; Zhao, J.; Liu, Z. Experimental investigation on characteristic parameters of air–water slug flow in a vertical tube. *Chem. Eng. Sci.* **2021**, *246*, 116895. [CrossRef]
45. Gokcal, B.; Al-Sarkhi, A.; Sarica, C.; Al-Safran, E.M. Prediction of slug frequency for high-viscosity oils in horizontal pipes. *SPE Proj. Facil. Constr.* **2010**, *5*, 136–144. [CrossRef]
46. Al-Lababidi, S. Multiphase Flow Measurement in the Slug Regime Using Ultrasonic Measurement Techniques and Slug Closure Model. Ph.D. Thesis, Cranfield University, Cranfield, UK, 2006.

47. Ruixi, D.; Da, Y.; Haihao, W.; Jing, G.; Ying, L.; Tong, Z.; Lijun, Z. Optical method for flow patterns discrimination, slug and pig detection in horizontal gas liquid pipe. *Flow Meas. Instrum.* **2013**, *32*, 96–102. [CrossRef]
48. Kouba, G.E. Horiozntal Slug Flow Modeling and Metering (Two-Phase Flow, Drift Velocity). Ph.D. Dissertation, The University of Tulsa, Tulsa, OK, USA, 1986.
49. Marcano, R.; Chen, X.T.; Sarica, C.; Brill, J.P. A study of slug characteristics for two-phase horizontal flow. In Proceedings of the SPE International Oil Conference and Exhibition in Mexico, Villahermosa, Mexico, 3–5 March 1998; SPE: Kuala Lumpur, Malaysia, 1998; p. SPE-39856.
50. Al-Safran, E. Investigation and prediction of slug frequency in gas/liquid horizontal pipe flow. *J. Pet. Sci. Eng.* **2009**, *69*, 143–155. [CrossRef]
51. Hernandez–Perez, V.; Abdulkadir, M.; Azzopardi, B. Slugging frequency correlation for inclined gas-liquid flow. *World Acad. Sci. Eng. Technol. Int. J. Chem. Mol. Eng.* **2010**, *4*, 10–17.
52. Farsetti, S.; Farisè, S.; Poesio, P. Experimental investigation of high viscosity oil–air intermittent flow. *Exp. Therm. Fluid Sci.* **2014**, *57*, 285–292. [CrossRef]
53. Picchi, D.; Manerba, Y.; Correra, S.; Margarone, M.; Poesio, P. Gas/shear-thinning liquid flows through pipes: Modeling and experiments. *Int. J. Multiph. Flow* **2015**, *73*, 217–226. [CrossRef]
54. Losi, G.; Arnone, D.; Correra, S.; Poesio, P. Modelling and statistical analysis of high viscosity oil/air slug flow characteristics in a small diameter horizontal pipe. *Chem. Eng. Sci.* **2016**, *148*, 190–202. [CrossRef]
55. Al-Ruhaimani, F.; Pereyra, E.; Sarica, C.; Al-Safran, E.; Chung, S.; Torres, C. A study on the effect of high liquid viscosity on slug flow characteristics in upward vertical flow. *J. Pet. Sci. Eng.* **2018**, *161*, 128–146. [CrossRef]
56. Dong, C.; Lu, L.; Wang, X. Experimental investigation on non-boiling heat transfer of two-component air-oil and air-water slug flow in horizontal pipes. *Int. J. Multiph. Flow* **2019**, *119*, 28–41. [CrossRef]
57. Almalki, N.; Ahmed, W.H. Evaluating the two-phase flow development through orifices using a synchronised multi-channel void fraction sensor. *Exp. Therm. Fluid Sci.* **2020**, *118*, 110165. [CrossRef]
58. dos Santos, E.N.; Schieck Reginaldo, N.; Longo, J.P.; da Fonseca, R., Jr.; Conte, M.G.; Morales, R.E.; Da Silva, M.J.J. Advancing oil and gas pipeline monitoring with fast phase fraction sensor. *Measure. Sci. Technol.* 2024, in press. [CrossRef]
59. Fossa, M.; Guglielmini, G.; Marchitto, A. Intermittent flow parameters from void fraction analysis. *Flow Meas. Instrum.* **2003**, *14*, 161–168. [CrossRef]
60. Saidj, F.; Hasan, A.; Bouyahiaoui, H.; Zeghloul, A.; Azzi, A. Experimental study of the characteristics of an upward two-phase slug flow in a vertical pipe. *Prog. Nucl. Energy* **2018**, *108*, 428–437. [CrossRef]
61. Ujang, P.M.; Lawrence, C.J.; Hale, C.P.; Hewitt, G.F. Slug initiation and evolution in two-phase horizontal flow. *Int. J. Multiph. Flow* **2006**, *32*, 527–552. [CrossRef]
62. Wang, X.; Guo, L.; Zhang, X. An experimental study of the statistical parameters of gas–liquid two-phase slug flow in horizontal pipeline. *Int. J. Heat Mass Transf.* **2007**, *50*, 2439–2443. [CrossRef]
63. Kadri, U.; Henkes, R.A.W.M.; Mudde, R.F.; Oliemans, R.V.A. A method for reducing the negative effects of long slugs. In Proceedings of the 7th North American Conference on Multiphase Technology, Banff, AB, Canada, 2–4 June 2010; OnePetro: Richardson, TX, USA, 2010.
64. Nair, J.; Pereyra, E.; Sarica, C. A statistical evaluation of slug frequency models for air-water flow in 6-in. ID near horizontal pipes. In Proceedings of the 10th North American Conference on Multiphase Technology, Banff, AB, Canada, 8–10 June 2016; OnePetro: Richardson, TX, USA, 2016.
65. Zhai, L.; Pu, G.; Meng, X.; Zhong, X. An investigation on hydrodynamic behavior of horizontal gas–liquid intermittent flow by S-PLIF and parallel-wire conductance sensors. *Chem. Eng. Sci.* **2024**, *301*, 120767. [CrossRef]
66. Kong, R.; Kim, S. Frequency of Plug/Slug Bubbles in Horizontal Air-Water Two-Phase Flow. In Proceedings of the International Conference on Nuclear Engineering, Virtual, Anaheim, CA, USA, 4–6 August 2021; American Society of Mechanical Engineers: New York, NY, USA, 2021; Volume 85253, p. V002T07A004.
67. Mi, Y.; Ishii, M.; Tsoukalas, L. Investigation of vertical slug flow with advanced two-phase flow instrumentation. *Nucl. Eng. Des.* **2001**, *204*, 69–85. [CrossRef]
68. Zhao, Y.; Yeung, H.; Lao, L. Slug frequency in high viscosity liquid and gas flow in horizontal pipes. In Proceedings of the 16th International Conference on Multiphase Production Technology, Cannes, France, 12–14 June 2013; BHR Group: Bedford, UK, 2013.
69. Abdulkadir, M.; Hernandez-Perez, V.; Lowndes, I.; Azzopardi, B.; Sam-Mbomah, E. Experimental study of the hydrodynamic behaviour of slug flow in a horizontal pipe. *Chem. Eng. Sci.* **2016**, *156*, 147–161. [CrossRef]
70. Dafyak, L.; Appah, D.; Onuoha, S.; Mukhtar, A. Effect of pipe inclination on the hydrodynamics of slug flow. In Proceedings of the SPE Nigeria Annual International Conference and Exhibition, Lagos, Nigeria, 6–8 August 2018; OnePetro: Richardson, TX, USA, 2018.
71. Omar, R.; Hewakandamby, B.; Azzi, A.; Azzopardi, B. Fluid structure behaviour in gas-oil two-phase flow in a moderately large diameter vertical pipe. *Chem. Eng. Sci.* **2018**, *187*, 377–390. [CrossRef]
72. Baba, Y.D.; Aliyu, A.M.; Archibong, A.-E.; Almabrok, A.A.; Igbafe, A.I. Study of high viscous multiphase phase flow in a horizontal pipe. *Heat Mass Transf.* **2018**, *54*, 651–669. [CrossRef]

73. Xu, Y.; Wang, H.; Cui, Z.; Dong, F. Application of electrical resistance tomography for slug flow measurement in gas/liquid flow of horizontal pipe. In Proceedings of the 2009 IEEE International Workshop on Imaging Systems and Techniques (IST), Shenzhen, China, 11–12 May 2009; IEEE: New York, NY, USA, 2009; pp. 319–323.
74. Pedersen, S.; Mai, C.; Hansen, L.; Durdevic, P.; Yang, Z. Online slug detection in multi-phase transportation pipelines using electrical tomography. *Ifac-Pap.* **2015**, *48*, 159–164. [CrossRef]
75. Heywood, N.; Richardson, J. Slug flow of air—Water mixtures in a horizontal pipe: Determination of liquid holdup by γ-ray absorption. *Chem. Eng. Sci.* **1979**, *34*, 17–30. [CrossRef]
76. El-Oun, Z. Gas-liquid two-phase flow in pipelines. In Proceedings of the SPE Annual Technical Conference and Exhibition, New Orleans, LA, USA, 23–26 September 1990; SPE-20645. SPE: Kuala Lumpur, Malaysia, 1990.
77. King, M.; Hale, C.; Lawrence, C.; Hewitt, G. Characteristics of flowrate transients in slug flow. *Int. J. Multiph. Flow* **1998**, *24*, 825–854. [CrossRef]
78. Odozi, U.A. Three-Phase Gas/Liquid/Liquid Slug Flow. Ph.D. Thesis, Imperial College of Science Technology and Medicine, London, UK, 2000.
79. Okezue, C.N. Application of the gamma radiation method in analysing the effect of liquid viscosity and flow variables on slug frequency in high viscosity oil-gas horizontal flow. *WIT Trans. Eng. Sci.* **2013**, *79*, 447–461.
80. Okezue, C. Evaluating the effects of high liquid viscosity and flow variables on horizontal oil–gas slug flows by gamma radiation method. *Int. J. Comput. Methods Exp. Meas.* **2014**, *2*, 374–391. [CrossRef]
81. Baba, Y.D.; Archibong, A.E.; Aliyu, A.M.; Ameen, A.I. Slug frequency in high viscosity oil-gas two-phase flow: Experiment and prediction. *Flow Meas. Instrum.* **2017**, *54*, 109–123. [CrossRef]
82. Ibarra, R.; Nossen, J.; Tutkun, M. Holdup and frequency characteristics of slug flow in concentric and fully eccentric annuli pipes. *J. Pet. Sci. Eng.* **2019**, *182*, 106256. [CrossRef]
83. Friedemann, C.; Mortensen, M.; Nossen, J. Two-phase flow simulations at 0− 4o inclination in an eccentric annulus. *Int. J. Heat Fluid Flow* **2020**, *83*, 108586. [CrossRef]
84. Kaji, R.; Azzopardi, B.; Lucas, D. Investigation of flow development of co-current gas–liquid vertical slug flow. *Int. J. Multiph. Flow* **2009**, *35*, 335–348. [CrossRef]
85. Vicencio, F.E.; Schneider, F.A.; Cozin, C.; Barbuto, F.A.; Da Silva, M.J.; Morales, R.E. An Experimental Characterization of Horizontal Gas-Liquid Slug Flow. In Proceedings of the ASME 2015 International Mechanical Engineering Congress and Exposition, Houston, TX, USA, 13–19 November 2015; American Society of Mechanical Engineers: New York, NY, USA, 2015; p. V07BT09A020.
86. Zhao, D.; Omar, R.; Abdulkadir, M.; Abdulkareem, L.; Azzi, A.; Saidj, F.; Perez, V.H.; Hewakandamby, B.; Azzopardi, B. The control and maintenance of desired flow patterns in bends of different orientations. *Flow Meas. Instrum.* **2017**, *53*, 230–242. [CrossRef]
87. Rodrigues, R.L.; Bertoldi, D.; dos Santos, E.N.; Schneider, F.A.; Neto, M.A.M.; da Silva, M.J.; Morales, R.E. Experimental analysis of downward liquid-gas slug flow in slightly inclined pipes. *Exp. Therm. Fluid Sci.* **2019**, *103*, 222–233. [CrossRef]
88. Conte, M.G.; Hegde, G.A.; da Silva, M.J.; Sum, A.K.; Morales, R.E. Characterization of slug initiation for horizontal air-water two-phase flow. *Exp. Therm. Fluid Sci.* **2017**, *87*, 80–92. [CrossRef]
89. Rosas, L.M.M.; Bassani, C.L.; Alves, R.F.; Schneider, F.A.; Neto, M.A.M.; Morales, R.E.M.; Sum, A.K. Measurements of horizontal three-phase solid-liquid-gas slug flow: Influence of hydrate-like particles on hydrodynamics. *AIChE J.* **2018**, *64*, 2864–2880. [CrossRef]
90. Rodrigues, R.L.; Cozin, C.; Naidek, B.P.; Neto, M.A.M.; da Silva, M.J.; Morales, R.E. Statistical features of the flow evolution in horizontal liquid-gas slug flow. *Exp. Therm. Fluid Sci.* **2020**, *119*, 110203. [CrossRef]
91. Barros, H.A.; Rodrigues, R.L.; Alves, R.F.; Cozin, C.; Rodrigues, H.T.; Junior, R.d.F.; da Silva, M.J.; Neto, M.A.M.; Morales, R.E. Experimental slug flow dissipation analysis in pipes with horizontal to inclined downward direction change. *Exp. Therm. Fluid Sci.* **2022**, *139*, 110740. [CrossRef]
92. Naidek, B.P.; Conte, M.G.; Cozin, C.; dos Santos, E.N.; Rodrigues, H.T.; Junior, R.d.F.; da Silva, M.J.; Morales, R.E. Experimental study of influence of liquid viscosity in horizontal slug flow. *Exp. Therm. Fluid Sci.* **2023**, *141*, 110798. [CrossRef]
93. Yu, H.-Y.; Xu, Q.; Cao, Y.-Q.; Huang, B.; Wang, H.-X.; Guo, L.-J. Characterizations of gas-liquid interface distribution and slug evolution in a vertical pipe. *Pet. Sci.* **2023**, *20*, 3157–3171. [CrossRef]
94. Silva, F.S.; Toledo, V.M.; Quinto, D.P.; Maya, J.C. Experimental slug flow characterization in a horizontal pipe. In *Experimental Heat Transfer, Fluid Mechanics and Thermodynamics*; Elsevier: Amsterdam, The Netherlands, 1997; pp. 893–900.
95. Woods, B.D.; Hanratty, T.J. Influence of Froude number on physical processes determining frequency of slugging in horizontal gas–liquid flows. *Int. J. Multiph. Flow* **1999**, *25*, 1195–1223. [CrossRef]
96. Jaeger, J.; Santos, C.; Rosa, L.; Meier, H.; Noriler, D. Experimental and numerical evaluation of slugs in a vertical air–water flow. *Int. J. Multiph. Flow* **2018**, *101*, 152–166. [CrossRef]
97. Wilkens, R.; Jepson, W.P. Studies of multiphase flow in high pressure horizontal and+ 5 degree inclined pipelines. In Proceedings of the Sixth International Offshore and Polar Engineering Conference, Los Angeles, CA, USA, 26–31 May 1996; OnePetro: Richardson, TX, USA, 1996.
98. Wilkens, R.J.; Thomas, D.K. A simple technique for determining slug frequency using differential pressure. *J. Energy Resour. Technol.* **2008**, *130*, 014501. [CrossRef]

99. Moré, P.P.; Kang, C.; Oliveira Magalhães, A.A. The Performance of Drag Reducing Agents in Multiphase Flow Conditions at High Pressure: Positive and Negative Effects. In Proceedings of the International Pipeline Conference, Calgary, AB, Canada, 29 September–3 October 2008; pp. 149–157.
100. Lin, M.; Liu, Y.; Hu, Y.; Che, D. Influence of the gas and liquid superficial velocity on slug frequency. *AIP Conf. Proc.* **2013**, *1547*, 253–263.
101. Wang, S.-Q.; Xu, K.-W.; Kim, H.-B. Slug flow identification using ultrasound Doppler velocimetry. *Int. J. Heat Mass Transf.* **2020**, *148*, 119004. [CrossRef]
102. Zhang, P.; Cao, X.; Qin, S.; Yin, P.; Guo, D.; Wu, C. Effect of SDS surfactant on gas-liquid flow and slug characteristics in slightly upward pipeline. *Int. J. Multiph. Flow* **2021**, *142*, 103695. [CrossRef]
103. Bamidele, O.E.; Hassan, M.; Ahmed, W.H. Flow induced vibration of two-phase flow passing through orifices under slug pattern conditions. *J. Fluids Struct.* **2021**, *101*, 103209. [CrossRef]
104. Thaker, J.; Banerjee, J. LDV as an Optical technique for Measurement of Plug/Slug Frequency in Gas-Liquid Two-Phase Flow. In *ASTFE Digital Library*; Begel House Inc.: Danbury, CT, USA, 2017.
105. Baungartner, R.; Gonçalves, G.; Loureiro, J.; Freire, A.S. Slug flows of gas and shear-thinning fluids in horizontal pipes. *Int. J. Multiph. Flow* **2023**, *165*, 104473. [CrossRef]
106. Errigo, M.; Windows-Yule, C.; Materazzi, M.; Werner, D.; Lettieri, P. Non-invasive and non-intrusive diagnostic techniques for gas-solid fluidized beds—A review. *Powder Technol.* **2023**, *431*, 119098. [CrossRef]
107. Sharaf, S.; Da Silva, M.; Hampel, U.; Zippe, C.; Beyer, M.; Azzopardi, B. Comparison between wire mesh sensor and gamma densitometry void measurements in two-phase flows. *Meas. Sci. Technol.* **2011**, *22*, 104019. [CrossRef]
108. Tian, D.; Yan, C.; Sun, L.; Tong, P.; Liu, G. Comparison of local interfacial characteristics between vertical upward and downward two-phase flows using a four-sensor optical probe. *Int. J. Heat Mass Transf.* **2014**, *77*, 1183–1196. [CrossRef]
109. Shi, X.; Tan, C.; Dong, F.; dos Santos, E.N.; da Silva, M.J. Conductance sensors for multiphase flow measurement: A review. *IEEE Sens. J.* **2020**, *21*, 12913–12925. [CrossRef]
110. Bieberle, A.; Windisch, D.; Iskander, K.; Bieberle, M.; Hampel, U. A smart multi-plane detector design for ultrafast electron beam X-ray computed tomography. *Sensors* **2020**, *20*, 5174. [CrossRef]
111. Gardenghi, Á.R.; Filho, E.d.S.; Chagas, D.G.; Scagnolatto, G.; Oliveira, R.M.; Tibiriçá, C.B. Overview of void fraction measurement techniques, databases and correlations for two-phase flow in small diameter channels. *Fluids* **2020**, *5*, 216. [CrossRef]
112. Ghendour, N.; Meribout, M.; Azzi, A. Review of measurement techniques for void fraction of two-phase flow through annulus. *Measurement* **2020**, *165*, 108196. [CrossRef]
113. Hampel, U.; Babout, L.; Banasiak, R.; Schleicher, E.; Soleimani, M.; Wondrak, T.; Vauhkonen, M.; Lähivaara, T.; Tan, C.; Hoyle, B.; et al. A review on fast tomographic imaging techniques and their potential application in industrial process control. *Sensors* **2022**, *22*, 2309. [CrossRef] [PubMed]
114. Wiedemann, P.; Dias, F.d.A.; Trepte, M.; Schleicher, E.; Hampel, U. Towards Real-Time Analysis of Gas-Liquid Pipe Flow: A Wire-Mesh Sensor for Industrial Applications. *Sensors* **2023**, *23*, 4067. [CrossRef] [PubMed]
115. Kipping, R.; Brito, R.; Scheicher, E.; Hampel, U. Developments for the application of the Wire-Mesh Sensor in industries. *Int. J. Multiph. Flow* **2016**, *85*, 86–95. [CrossRef]
116. Wiedemann, P.; Dias, F.d.A.; Schleicher, E.; Hampel, U. Temperature compensation for conductivity-based phase fraction measurements with wire-mesh sensors in gas-liquid flows of dilute aqueous solutions. *Sensors* **2020**, *20*, 7114. [CrossRef]
117. Garcia, M.M.; Sattar, M.A.; Atmani, H.; Legendre, D.; Babout, L.; Schleicher, E.; Hampel, U.; Portela, L.M. Towards Tomography-Based Real-Time Control of Multiphase Flows: A Proof of Concept in Inline Fluid Separation. *Sensors* **2022**, *22*, 4443. [CrossRef]
118. Jia, J.; Babatunde, A.; Wang, M. Void fraction measurement of gas–liquid two-phase flow from differential pressure. *Flow Meas. Instrum.* **2015**, *41*, 75–80. [CrossRef]
119. Wu, K.; Galli, F.; de Tommaso, J.; Patience, G.S.; van Ommen, J.R. Experimental methods in chemical engineering: Pressure. *Can. J. Chem. Eng.* **2023**, *101*, 41–58. [CrossRef]
120. Yadigaroglu, G.; Hewitt, G.F. (Eds.) *Introduction to Multiphase Flow: Basic Concepts, Applications and Modelling*; Springer: Berlin/Heidelberg, Germany, 2018.
121. Campos, J.B.L.M.; De Carvalho, J.R.F.G. An experimental study of the wake of gas slugs rising in liquids. *J. Fluid Mech.* **1988**, *196*, 27–37. [CrossRef]
122. Nydal, O.J. An Experimental Investigation on Slug Flow. Ph.D. Thesis, University of Oslo, Oslo, Norway, 1991.
123. Abdulkadir, M.; Hernandez-Perez, V.; Lowndes, I.; Azzopardi, B.; Dzomeku, S. Experimental study of the hydrodynamic behaviour of slug flow in a vertical riser. *Chem. Eng. Sci.* **2014**, *106*, 60–75. [CrossRef]
124. Eyo, E.N.; Lao, L. Slug flow characterization in horizontal annulus. *AIChE J.* **2019**, *65*, e16711. [CrossRef]
125. Abdul Basith, M.S.; Sallih, N.; Soon, W.P.K.; Shibano, S.T.; Singh, R.; Sulong, M.A. Effects of Selection of Inlet Perturbations, Multiphase and Turbulence Equations on Slug Flow Characteristics Using Altair® AcuSolve™. *Processes* **2021**, *9*, 2152. [CrossRef]
126. Manolis, I.G. High Pressure Gas-Liquid Slug Flow. Doctoral Dissertation, Imperial College, London, UK, 1995.
127. Archibong, A. Viscous Multiphase Flow Characteristics in Pipelines. Ph.D. Thesis, Cranfield University, Cranfield, UK, 2015.
128. Schmelter, S.; Olbrich, M.; Schmeyer, E.; Bär, M. Numerical simulation, validation, and analysis of two-phase slug flow in large horizontal pipes. *Flow Meas. Instrum.* **2020**, *73*, 101722. [CrossRef]

129. Schmelter, S.; Knotek, S.; Olbrich, M.; Fiebach, A.; Bär, M. On the influence of inlet perturbations on slug dynamics in horizontal multiphase flow—A computational study. *Metrologia* **2021**, *58*, 014003. [CrossRef]
130. Archibong-Eso, A.; Baba, Y.; Aliyu, A.; Zhao, Y.; Yan, W.; Yeung, H. On slug frequency in concurrent high viscosity liquid and gas flow. *J. Pet. Sci. Eng.* **2018**, *163*, 600–610. [CrossRef]
131. Drew, T.B.; Koo, E.C.; McAdams, W.H. The friction factor for clean round pipes. *Trans. AIChE* **1932**, *28*, 56–72.
132. Ujang, P.M. Studies of Slug Initiation and Development in Two-Phase Gas-Liquid Pipeline Flow. Doctoral Dissertation, Imperial College London, London, UK, 2003.
133. Soto-Cortes, G.; Pereyra, E.; Sarica, C.; Torres, C.; Soedarmo, A. Signal processing for slug flow analysis via a voltage or instantaneous liquid holdup time-series. *Flow Meas. Instrum.* **2021**, *79*, 101968. [CrossRef]
134. Bressani, M.; Mazza, R.A. Two-phase slug flow through an upward vertical to horizontal transition. *Exp. Therm. Fluid Sci.* **2018**, *91*, 245–255. [CrossRef]
135. Al-Safran, E.M. An Experimental and Theoretical Investigation of Slug Flow Characteristics in the Valley of a Hilly-Terrain Pipeline. Ph.D. Thesis, The University of Tulsa, Tulsa, OK, USA, 2003.
136. Soedarmo, A.A.; Rodrigues, H.T.; Pereyra, E.; Sarica, C. A new objective and distribution-based method to characterize pseudo-slug flow from wire-mesh-sensors (WMS) data. *Exp. Therm. Fluid Sci.* **2019**, *109*, 109855. [CrossRef]
137. Soto-Cortes, G.; Pereyra, E.; Sarica, C.; Torres, C.; Soedarmo, A. Signal processing for slug flow analysis: MATLAB algorithm. *MethodsX* **2021**, *8*, 101546. [CrossRef]
138. Yoon, D.; Hayashi, T.; Park, H.J.; Tasaka, Y.; Murai, Y.; Takano, S.; Masanobu, S. Ultrasound measurement of large bubbles rising in angled slug pipe flows. *Flow Meas. Instrum.* **2023**, *91*, 102357. [CrossRef]
139. Van Ommen, J.R.; Sasic, S.; Van der Schaaf, J.; Gheorghiu, S.; Johnsson, F.; Coppens, M.O. Time-series analysis of pressure fluctuations in gas–solid fluidized beds–A review. *Int. J. Multiph. Flow* **2011**, *37*, 403–428. [CrossRef]
140. Alamu, M.B.; Azzopardi, B.J. Flow pattern and slug dynamics around a flow splitter. *J. Fluids Eng.* **2011**, *133*, 121105. [CrossRef]
141. Ahmed, W.H. Experimental investigation of air–oil slug flow using capacitance probes, hot-film anemometer, and image processing. *Int. J. Multiph. Flow* **2011**, *37*, 876–887. [CrossRef]
142. Vince, M.A.; Lahey, R.T., Jr. On the development of an objective flow regime indicator. *Int. J. Multiph. Flow* **1982**, *8*, 93–124. [CrossRef]
143. Solomon, O.M., Jr. PSD computations using Welch's method. In *NASA STI/Recon Technical Report N, 92*; Sandia National Lab. (SNL-NM): Albuquerque, NM, USA, 1991; p. 23584.
144. Kesana, N.R.; Vieira, R.; Schleicher, E.; McLaury, B.S.; Shirazi, S.A.; Hampel, U. Experimental study of slug characteristics: Implications to sand erosion. In Proceedings of the Fluids Engineering Division Summer Meeting, Incline Village, NV, USA, 7–11 July 2013; American Society of Mechanical Engineers: New York, NY, USA, 2013; Volume 55560, p. V01CT17A007.
145. Akhlaghi, M.; Taherkhani, M.; Nouri, N.M. Study of intermittent flow characteristics experimentally and numerically in a horizontal pipeline. *J. Nat. Gas Sci. Eng.* **2020**, *79*, 103326. [CrossRef]
146. Soedarmo, A.A. Gas-Oil Flow in Upward-Inclined Pipes: Pseudo-Slug Flow Modeling and Upscaling Studies. Ph.D. Thesis, The University of Tulsa, Tulsa, OK, USA, 2019.
147. Vieira, S.C.; Fabro, A.T.; Rodrigues, R.L.; da Silva, M.J.; Morales, R.E.; Castro, M.S. A two-state Markov chain model for slug flow in horizontal ducts. *Flow Meas. Instrum.* **2023**, *90*, 102335. [CrossRef]
148. Henry, M. An ultra-precise Fast Fourier Transform. *Measurement* **2023**, *220*, 113372. [CrossRef]
149. Hernandez-Perez, V. Gas-Liquid Two-Phase Flow in Inclined Pipes. Ph.D. Thesis, University of Nottingham, Nottingham, UK, 2007.
150. Azzopardi, B.; Do, H.; Azzi, A.; Perez, V.H. Characteristics of air/water slug flow in an intermediate diameter pipe. *Exp. Therm. Fluid Sci.* **2015**, *60*, 1–8. [CrossRef]
151. Mudde, R.F.; Saito, T. Hydrodynamical similarities between bubble column and bubbly pipe flow. *J. Fluid Mech.* **2001**, *437*, 203–228. [CrossRef]
152. Azzopardi, B.; Zhao, D.; Yan, Y.; Morvan, H.; Mudde, R.F.; Lo, S. *Hydrodynamics of Gas-Liquid Reactors: Normal Operation and Upset Conditions*; John Wiley & Sons: Hoboken, NJ, USA, 2011.
153. Besagni, G. Bubble column fluid dynamics: A novel perspective for flow regimes and comprehensive experimental investigations. *Int. J. Multiph. Flow* **2021**, *135*, 103510. [CrossRef]
154. Kouzbour, S.; Gourich, B.; Stiriba, Y.; Vial, C.; Gros, F.; Sotudeh-Gharebagh, R. Experimental analysis of the effects of liquid phase surface tension on the hydrodynamics and mass transfer in a square bubble column. *Int. J. Heat Mass Transf.* **2021**, *170*, 121009. [CrossRef]
155. Woods, B.D.; Fan, Z.; Hanratty, T.J. Frequency and development of slugs in a horizontal pipe at large liquid flows. *Int. J. Multiph. Flow* **2006**, *32*, 902–925. [CrossRef]
156. Luo, X.M.; He, L.M.; Lu, Y.L. Fluctuation characteristics of gas-liquid two-phase slug flow in horizontal pipeline. *AIP Conf. Proc.* **2010**, *1207*, 162–171.
157. Arabi, A.; Salhi, Y.; Zenati, Y.; Si-Ahmed, E.-K.; Legrand, J. Identifying the intermittent flow sub-regimes using pressure drop time series fluctuations. *Exp. Comput. Multiph. Flow* **2024**, *6*, 28–40. [CrossRef]